

Mixed Color Emission from Europium Co-Doped $\text{La}_2\text{O}_3:\text{Bi}^{3+}$ Nanophosphors Material by Polyol Method



Physics

KEYWORDS : Polyol method, Lanthanum oxide, Bismuth, Rare earth co-doping, Phosphorous, Photoluminescence.

*P.V.S.S.N.Reddy

Crystal Growth and Nanoscience Research Centre, Department of Physics, Government College (A), Rajahmundry-533105, A.P. India. * corresponding author

K.Sujatha

Crystal Growth and Nanoscience Research Centre, Department of Physics, Government College (A), Rajahmundry-533105, A.P. India.

Ch.Satya Kamal

Crystal Growth and Nanoscience Research Centre, Department of Physics, Government College (A), Rajahmundry-533105, A.P. India.

T.Samuel

Crystal Growth and Nanoscience Research Centre, Department of Physics, Government College (A), Rajahmundry-533105, A.P. India.

M.Indiradevi

Department of Physics, Andhra University, Visakhapatnam-A.P, India

K.Ramachandra Rao*

Crystal Growth and Nanoscience Research Centre, Department of Physics, Government College (A), Rajahmundry-533105, A.P. India. *Corresponding Author

ABSTRACT

Photoluminescence (PL) was observed from prepared Bi^{3+} and europium (Eu^{3+}) co-doped La_2O_3 ($\text{La}_2\text{O}_3:\text{Bi}, \text{Eu}$) nanophosphor powder. The phosphor powders were prepared by polyol method using ethylene glycol as capping agent. The phase formation, functional groups identification of as prepared samples and morphological studies were confirmed by XRD, FTIR and scanning electron microscopy (SEM) and transmission electron microscopy (TEM). PL emission widely changed from green-orange region to approximately blue on heating $\text{La}_2\text{O}_3:\text{Bi}^{3+}, \text{Eu}^{3+}$ phosphor powders from 700 to 900 °C. The observed emission peaks in PL from phosphor powder materials were assigned to either the broad emission originating from the transition in Bi^{3+} or the visible emission peaks originating transition from the europium ion. Emission peaks of PL are plotted using CIE coordinates.

INTRODUCTION

Rare earth doped La_2O_3 phosphors have many potential applications in cathode ray tubes, field emission displays, plasma display panels, and vacuum fluorescent display devices [1]. Among various phosphors, materials doped with bismuth ions (Bi^{3+}) have extensively investigated because Bi^{3+} is to be good sensitizers of luminescence due to their band-like absorption character. In using rare-earth (RE) sesquioxides $\text{La}_2\text{O}_3, \text{Y}_2\text{O}_3, \text{Gd}_2\text{O}_3$ as host materials and doped with Bi^{3+} ions, it has been observed that blue-violet emissions arose from these phosphors [2-4]. Lanthanum oxide (La_2O_3) is a semiconductor material [5] with the largest band gap among RE sesquioxides, with a value of 4.3 eV [6]. Red phosphors like Eu^{3+} activated phosphors have been extensively investigated in the field of their application [7-10]. Furthermore, Eu^{3+} is often used as a structural probe [11], because of the relative simplicity of its energy-level structure and the fact that it possesses non-degenerate ground (7F_0) and excited (5D_0) states, and because the absorption and emission spectra of this ion show marked dependence on its site symmetry in the host material [12]. Photoluminescence (PL) and electroluminescence (EL) were observed from rare earth (RE^{3+}) co-doped $\text{La}_2\text{O}_3:\text{Bi}^{3+}$ ($\text{La}_2\text{O}_3:\text{Bi}^{3+}, \text{RE}^{3+}$) phosphor thin films [13]. Many preparation techniques such as calcination methods [14], solutions combustion synthesis [15-17], conventional hydrothermal [18] and microwave hydrothermal methods [19] used for preparation of La_2O_3 nanoparticles. To the best of authors knowledge, $\text{La}_2\text{O}_3:\text{Bi}^{3+}$, co-doped with Eu^{3+} ions ($\text{La}_2\text{O}_3:\text{Bi}^{3+}, \text{Eu}^{3+}$) nanoparticles synthesized by polyol route have not yet been investigated so far.

Polyol method can be used to prepare a variety of materials/compounds including metals, oxides, phosphates, sulphides, fluorides etc. having size in the range of few nanometers to micrometers. Essentially the preparation method involves the reaction of a polyol soluble salt of the metal ions and a precipitating agent. The method offers simple and economic method without using any

hazardous or moisture sensitive reagents for preparing a variety of nanomaterials. In this paper, novel $\text{La}_2\text{O}_3:\text{Bi}^{3+}, \text{Eu}^{3+}$ nanoparticles were prepared successfully followed by annealing at 700 °C and 900 °C temperatures and their luminescent properties were discussed in detail.

EXPERIMENTAL DETAILS

Preparation of the nanoparticles

Starting materials, $\text{La}(\text{NO}_3)_3 \cdot 6\text{H}_2\text{O}$ [Merck, Germany], $\text{Bi}(\text{NO}_3)_3 \cdot 5\text{H}_2\text{O}$ [BDH Laboratory Chemicals Division, India], $\text{Eu}(\text{NO}_3)_3$ [Alfa Aesar 99.99%], were used for the synthesis of nanoparticles. All the reagents were of AR and were used without further purification. Here ethylene glycol is used as the capping agent and urea for hydrolysis. Initially $\text{La}_2\text{O}_3:\text{Bi}^{3+}$ (1at %) nanoparticles were prepared. Both $\text{La}(\text{NO}_3)_3 \cdot 6\text{H}_2\text{O}$ and $\text{Bi}(\text{NO}_3)_3 \cdot 5\text{H}_2\text{O}$ were dissolved in required amount of distilled water. To this solution, ethylene glycol (25 mL) was added and it was then transferred into a two-necked RB flask. The solution was slowly heated up to 100 °C followed by addition of 2 g of urea and the temperature was increased to 120 °C. At this temperature, the solution became turbid. The temperature was maintained at this value for 2 hours. The precipitate was collected after the reaction by centrifugation and then washed two times with acetone and three times with methanol followed by drying under ambient conditions. The samples prepared thus were finally heated to 700 °C, 900 °C in air at a heating rate of 10 °C per minute. The temperature was maintained at the respective values for duration of 5 hours. After that the furnace was switched off and the sample was subjected to natural cooling to room temperature. The same procedure was used for preparing the rare-earth co-doped $\text{La}_2\text{O}_3:\text{Bi}^{3+}, \text{Eu}^{3+}$ nanoparticles. Along with $\text{La}(\text{NO}_3)_3 \cdot 6\text{H}_2\text{O}$ and $\text{Bi}(\text{NO}_3)_3 \cdot 5\text{H}_2\text{O}$, $\text{Eu}(\text{NO}_3)_3$ was also added. Here in this paper the 1 at % bismuth content is added and 1 at% optimum europium is reported for co-doping due to concentration quenching effect.

Characterization

X-ray diffraction (XRD) studies were carried out using a Philips powder X-ray diffract meter (model PW 1071) with Ni filtered Cu-K α radiation. The lattice parameters, unit cell volume were obtained from Rietveld refinement of the XRD patterns using POWDERX software. The average crystallite size was calculated from the diffraction line width based on Scherrer relation $D = 0.9\lambda/\beta\cos\theta$, where D is the average particles size, λ is the wavelength of X-rays and β is the corrected full width at half maximum (FWHM). All luminescence measurements were carried out at room temperature with a resolution of 5 nm, using Edinburgh Instruments FLSP 920 system attached with a 450 W Xe lamp as the excitation source. A micro second flash lamp was used for lifetime measurements. Transmission Electron Microscopic (TEM) studies were performed using a JEOL JEM 3000F TEM machine. IR patterns were recorded for a thin pellet of the La₂O₃:Bi³⁺, Tb³⁺ as prepared nanoparticles made with KBr using a Bomem MB102 machine.

RESULTS AND DISCUSSION

XRD Analysis

The phase of the as-prepared undoped La(OH)₃ and doped samples was examined by XRD. Fig.1 (a) shows the XRD patterns of the pure La(OH)₃ sample which all the diffraction peaks are attributed to the hexagonal crystal phase, which are in good agreement with the standard PCPDF card [13-0084] with the space group P6₃/m. Initially upon heating to 700 °C the XRD peaks became sharper because of an increase in crystallinity. With increasing temperature, it was deduced that La(OH)₃ transforms to La₂O₃. This XRD peaks shows the oxide nanoparticle phase which is in almost close agreement with hexagonal phase (PCPDF 83-1355) with the space group Pm1 Fig.1 (b) [20]

Fig.1 XRD Pattern for as prepared La₂O₃ (a) and 700 °C heated undoped La₂O₃ (b) La₂O₃:Bi³⁺ (c) Co-doped with (d) Eu³⁺

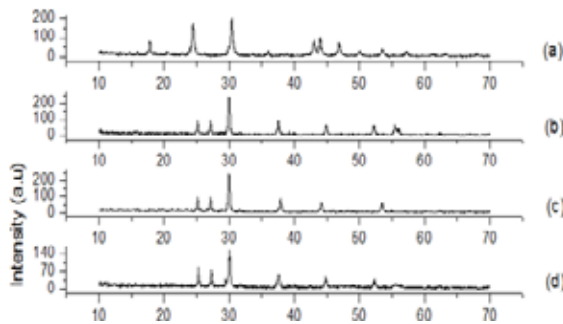
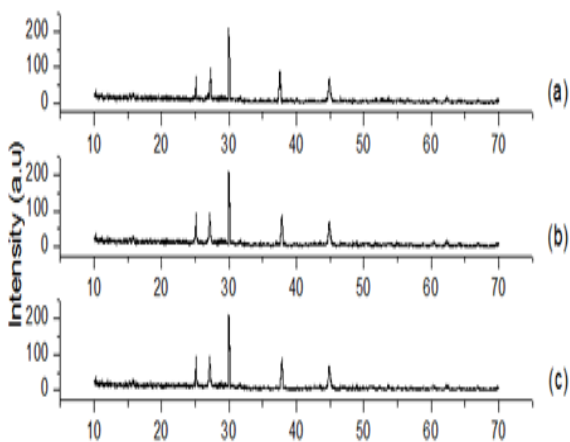
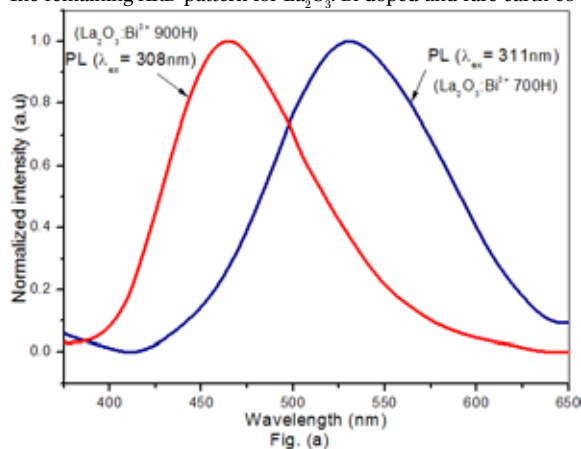


Fig.2 XRD Pattern for 900 °C heated undoped La₂O₃ (a)



La₂O₃:Bi³⁺ (b) Co-doped with (c) Eu³⁺

The remaining XRD pattern for La₂O₃:Bi doped and rare earth co-



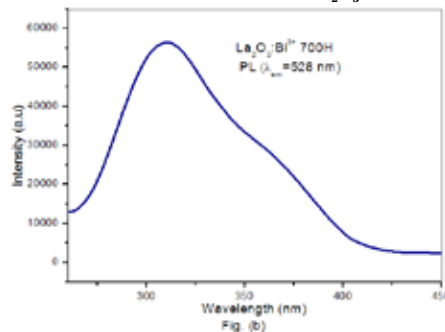
doped samples Fig 1. (a and d) are indexed with the hexagonal form of La₂O₃. For getting pure hexagonal crystal structure, high temperature heating is done at 900 °C. Hence pure hexagonal phase is attributed with better crystallinity. Fig.2 (a-c) shows 900 °C undoped La₂O₃, La₂O₃:Bi³⁺ and Eu³⁺ co-doped La₂O₃:Bi³⁺. No diffraction peaks of other impurities were detected, even when co-doping is done to La₂O₃:Bi³⁺. From Figs.1 and 2 a slight shift in peaks is observed due to co-doping. From this result it is noticed that the doped Eu³⁺ and Bi³⁺ ions completely enter into the matrix and occupy La³⁺ sites in these phosphors. According to the Scherrer's equation, the average crystallite size of heated samples is estimated to be 32- 39 nm. The cell parameters of the heated samples at 700 °C and 900 °C have also been determined by X-ray diffraction and refined using the POWDERX software. The cell parameters calculated were listed in Table.1 minor changes are observed in lattice parameters on co-doping. Lattice parameters of La₂O₃ for reference are a= 4.057 Å =b and c= 6.430 Å.

**TABLE - 1 & 2
CELL PARAMETERS OF HEATED SAMPLES**

Sample	700 °C Heated			
	a (Å)	b (Å)	c (Å)	V(cc)
Undoped La ₂ O ₃	4.021(3)	4.021(3)	6.541(3)	91.63
La ₂ O ₃ : Bi ³⁺	4.018(8)	4.018(8)	6.497(8)	90.54
La ₂ O ₃ :Bi ³⁺ ,Eu ³⁺	4.027(3)	4.027(3)	6.488(3)	91.16

Sample	900 °C Heated			
	a (Å)	b (Å)	c (Å)	V(cc)
Undoped La ₂ O ₃	4.023(3)	4.023(3)	6.552(3)	91.44
La ₂ O ₃ : Bi ³⁺	4.026(2)	4.026(2)	6.517(3)	91.31
La ₂ O ₃ :Bi ³⁺ ,Eu ³⁺	4.029(4)	4.029(4)	6.510(4)	91.54

PL studies from 1 at% Bi doped La₂O₃ powder phosphors



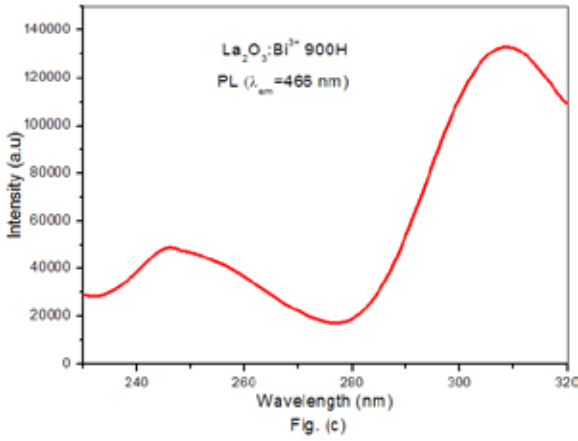


Fig.3 PL emission spectra (a) La₂O₃:Bi³⁺ 700 and 900 °C heated samples (b) PL excitation spectra La₂O₃:Bi³⁺ 700° C heated and (c) PL excitation spectra La₂O₃:Bi³⁺ 900 °C heated samples.

Blue emission from La₂O₃: Bi³⁺ phosphor thin film has been previously reported [21–23]. The emission spectra of 700 and 900 °C heated La₂O₃:Bi³⁺ powder samples are shown Fig.3 (a). The emission peak maximum at 528nm of 700 °C heated sample under excitation of 311nm is observed and corresponding excitation spectra is shown in Fig.3 (b). As for the 900°C sample it is observed a blue shift in emission peak at 466nm and increase in emission intensity when excited at 308nm. During sintering, excited luminescent centers are thermally activated through phonon interactions, which cause thermal release through the crossing point between the excited and ground states according to a configuration coordinate diagram [24].

At higher temperature, the density of phonons increases and electron-phonon interactions dominate, so a blue shift of the emission band is observed for the phosphors as the temperature increases which is in accord with the reported thin film La₂O₃:Bi³⁺ phosphor [25]. In general, the temperature dependence of phosphors used in phosphor-conversion white LEDs is important because it has a considerable influence on the light output and color rendering index. From Fig.3 (c) the excitation spectra of 900 °C consists of two bands, the main excitation band peaks around 308 nm and the weak band peaks around 250 nm, originating from the 6s²–6sp transition in Bi³⁺.

The lifetime value is found to be significantly lower (0.9 μs) for 700 °C heated sample when compared to the 900 °C sample (8.2 μs) which can be seen from the decay curve shown in Fig. 4(a, b) This is explained based on the general expression for the oscillator strength of an electronic transition (f_{ox}), as given by equation 1, [26]

$$f_{ox} = \frac{2m}{\hbar} \Delta E |\mu|^2 |U(0)|^2 \dots\dots\dots (1)$$

Where ΔE is the transition energy, μ is the transition dipole moment and |U(0)|² is the probability of finding an electron and hole at the same place, m is the effective mass of electron, and h is Planks constant. For nanoparticles, due to their small size, the term, |U(0)|² is much higher compared to corresponding bulk and hence will have higher transition probability with respect to bulk. Higher oscillator strength (f_{ox}) values suggest shorter excited state lifetime, as both are inversely related. This accounts for the observed decrease in the lifetime values for the 700 °C samples compared to corresponding 900 °C samples. Since the decays are multi exponential average lifetime values are calculated and used for comparison.

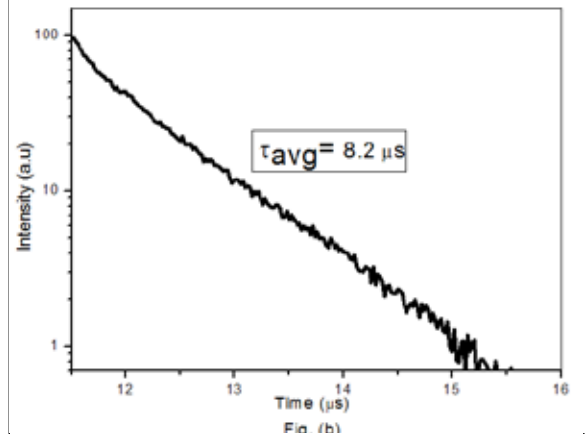
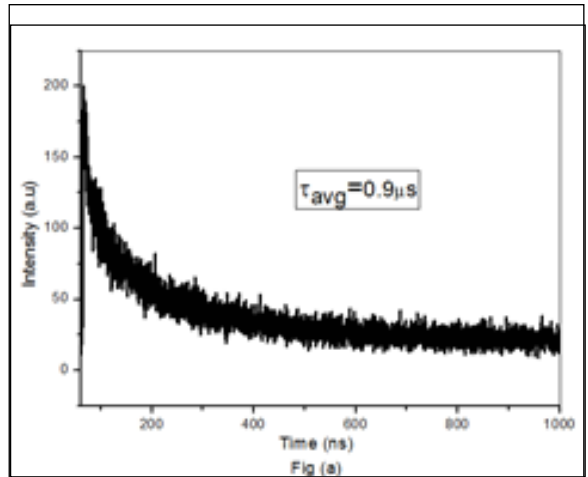


Fig.4 Decay curves corresponding to (a) La₂O₃:Bi³⁺ (700 °C) heated and (b) La₂O₃:Bi³⁺ (900 °C) heated samples.

PL studies from La₂O₃:1 at % Bi, 1 at% Eu powder phosphor

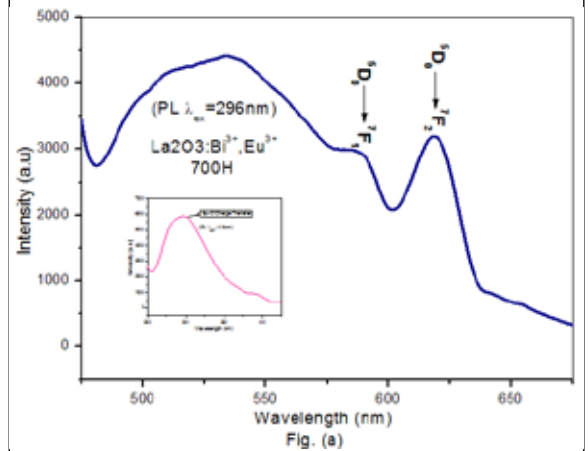
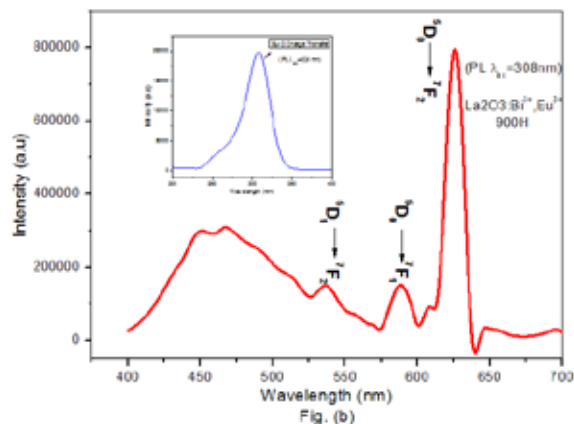


Fig.5 (a, b) shows the excitation and emission spectra of the 700 °C and 900 °C heated Eu³⁺doped samples. For the excitation spectra Fig. 5 (a) (inset) of the 700 °C (1 at%) Eu³⁺ co-doped sample emission is monitored at 616 nm. Eu–O CT transition band centred at around 296 nm is observed. For the emission spectra (excited at 296 nm) emission peaks centred at 589, 616 nm are ascribed to Eu³⁺ 4f transitions from the excited level ⁵D₀ --- ⁷F₂, ⁵D₀ --- ⁷F₁ in which the strongest emission band at 616 nm is attributed to the transition ⁵D₀ --- ⁷F₂ [27]. Whereas for excitation spectra Fig.5 (b) (inset) of 900 °C heated Eu³⁺ co-doped (1 at%) sample, Eu–O CT transition band centred at around 626

nm is observed. It is noticed that due to the presence of Bi³⁺ ions O²⁻ and Eu³⁺ electron (f-f) transitions are almost null.



In general two excitation bands ranging from 230–275 nm and 275–350 nm are to be observed in La₂O₃:Bi³⁺ doped samples, but with addition of Eu³⁺ the host absorption band centred at 250 nm nearly disappears in both the heated samples. Emission spectra Fig. 5(b) of 900 °C heated sample excited at 308 nm emission peaks centred at 536, 589, 616 nm are ascribed to Eu³⁺ 4f transitions from the excited level ⁵D₁ --- ⁷F₂, ⁵D₀ --- ⁷F₂, ⁵D₀ --- ⁷F₂ in which the strongest emission band at 626 nm is attributed to the transition ⁵D₀ --- ⁷F₂. According to spectra it clearly shows that as on heating to higher temperature the peak intensities increases dramatically due to an increase in crystallinity and a decrease in the number of quenching sites (e.g., adsorbed OH). The OH group quenches the luminescence via non-radiative relaxation processes [28]. For this reason, thermal annealing could eliminate the quenching sites to increase the luminescence efficiency. This result indicates the existence of efficient energy transfer between the Bi³⁺ and Eu³⁺ ions in 900 °C heated sample is more when compared with 700°C heated sample. The corresponding multi exponential life time decay curves are shown in Fig. 6 (a, b) The average life time values of 900 °C and 700 °C heated sample found to be τ_{avg} = 2.13ms and τ_{avg} = 1.09 ms

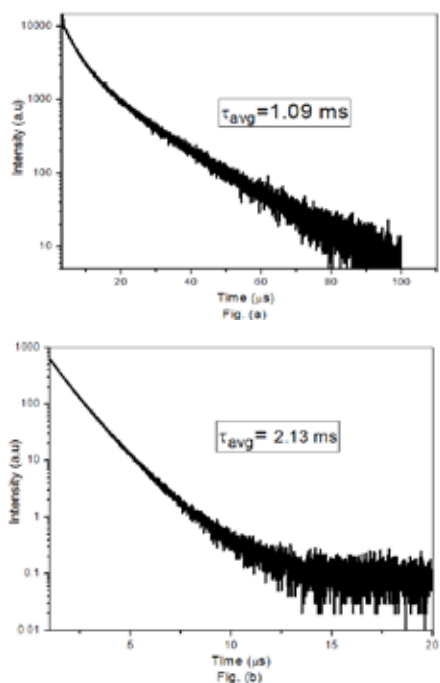
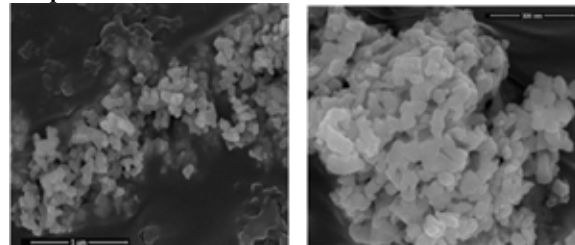


Fig.6-Decay curves corresponding to (a) La₂O₃:Bi³⁺,Eu³⁺ (700 °C) heated and (b) La₂O₃:Bi³⁺, Eu³⁺ (900 °C) heated samples.

Structural and morphological studies

SEM

Fig.7 SEM images of La₂O₃ 700 °C heated Undoped and Doped Samples



(a) Undoped La₂O₃ (b) La₂O₃: Bi³⁺

(c) La₂O₃: Bi³⁺, Eu³⁺

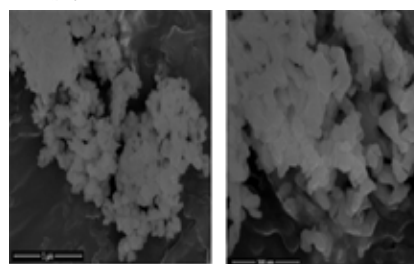
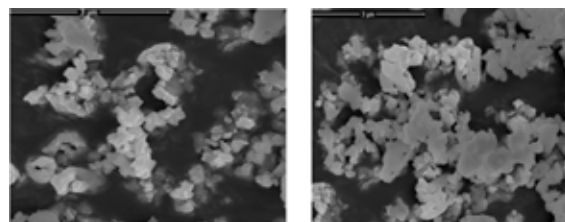


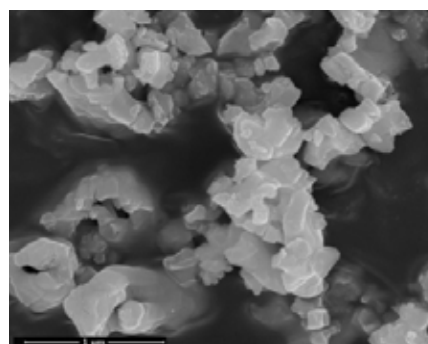
Fig. 8 SEM images of La₂O₃ 900 °C heated Undoped and Doped Samples



(a)Undoped La₂O₃ (b) La₂O₃: Bi³⁺

(c) La₂O₃: Bi³⁺, Eu³⁺

The surface morphology and crystallinity of solid host materials are important parameters which determine the emission characteristics of phosphors. The morphological analysis of La₂O₃, La₂O₃:Bi³⁺ and rare earth co-doped heated at 700 and 900 °C samples was performed by SEM examination shown in Figs 7 and 8. It can be seen from images the samples are of sphere-like structure. From these images it is clear that the aggregation and particle sizes of the La₂O₃: Bi³⁺ increases with Eu³⁺ co-doping. Also, it is clearly seen that the particles are in the agglomerated form with their size in the micrometer range.



TEM Fig. 9 (a) TEM image (b) SAED pattern (c) HRTEM of 700 °C La₂O₃: Bi³⁺, Eu³⁺ phosphors material

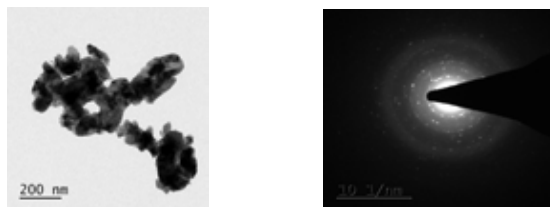
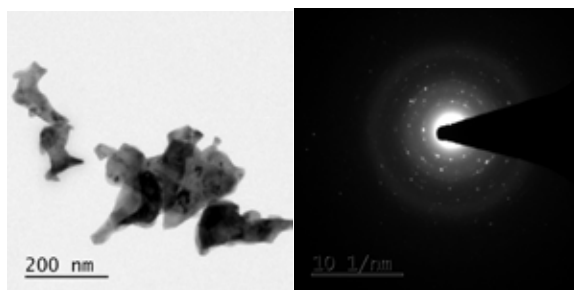
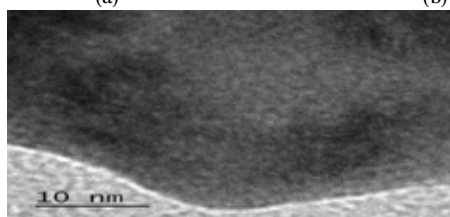


Fig. 10 (a) TEM image (b) SAED pattern (c) HRTEM of 900 °C $\text{La}_2\text{O}_3 : \text{Bi}^{3+}, \text{Eu}^{3+}$ phosphors material



(a) (b)

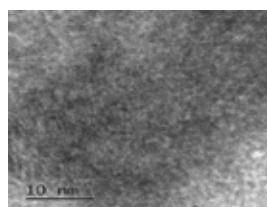
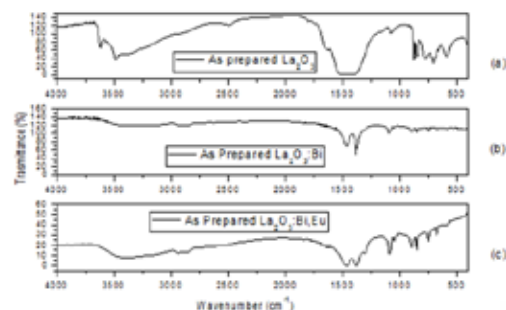


(c)

Fig.9 (a)–(c) represents TEM, SAED patterns, HRTEM image of $\text{La}_2\text{O}_3:\text{Bi}^{3+}, \text{Eu}^{3+}$ sample after heating at 700 °C which indicates the created oxides are nanocrystalline materials with the average crystalline grain size of about 40-50nm which slightly more when compared with size calculated from Scherrer’s relation in XRD. When the calcination temperature was further increased to 900 °C, the nanoparticles became bigger and merged with each other, and the sharpness of the particles completely vanished. The merging is related to the melting process because the surface-to-volume ratio of the nanoparticles is relatively high, and at high temperatures, the surface energy substantially affects the interior bulk properties of the materials. Fig. 10 (a-c) shows TEM, SAED patterns, HRTEM image of 900 °C. The fine structure of 700 and 900 °C $\text{La}_2\text{O}_3 : \text{Bi}^{3+}, \text{Eu}^{3+}$ samples was further studied from the HRTEM images and SAED patterns. The SAED patterns of the heated samples confirmed their nanocrystalline nature by producing a number of bright spots in an irregular manner.

FTIR Spectra

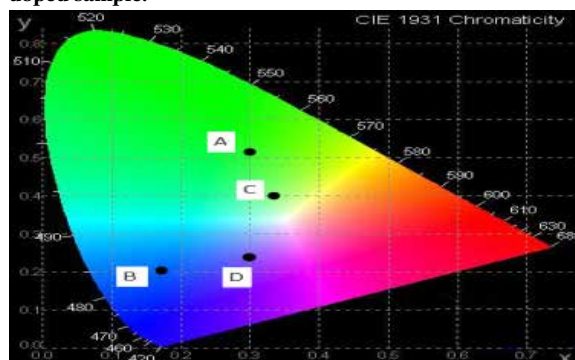
FT-IR spectrum of as-prepared dried samples recorded from 400 to 4000 cm^{-1} shown in Fig.11. The as prepared (undoped) La_2O_3



spectrum Fig.(a) shows a sharp band at 3614 cm^{-1} , corresponding to the stretching and bending O–H vibrations [29] and absorption band at 3481 cm^{-1} results from the O–H vibration of H_2O absorbed by the nanoparticles. The strong broad band at 1450 cm^{-1} is attributed to C-H bending. The FT-IR spectrum is in good agreement with the XRD pattern of as prepared La_2O_3 . Whereas from the spectra Fig. 11 (b, c) of $\text{La}_2\text{O}_3 : \text{Bi}^{3+}$ doped and europium co-doped samples it is clearly shows the absence of sharp peak at 3614 cm^{-1} [30, 31]. The weak absorption band peak observed at O-H vibration of water molecules that are absorbed by bismuth doped nanoparticles at 3471 cm^{-1} and weak broad band assigned at 3462 cm^{-1} for co-doped samples. A medium C-H bond stretching is observed at 2892 cm^{-1} and two peaks were commonly observed at 1384 and 1464 cm^{-1} , which were assigned C-H bending, respectively in all doped La_2O_3 nanoparticles. Hence, the doped Bi^{3+} and europium ions are soluble in ethylene glycol (EG) homogenously by forming steady metal complexes due chelation between metal ions and EG which is verified from IR spectra.

Fig. 11 FTIR spectra of As Prepared $\text{La}_2\text{O}_3:\text{Bi}^{3+}, \text{Eu}^{3+}$ CIE Coordinates

Fig. 12 CIE chromaticity color coordinates in PL emissions from 700 °C and 900 °C heated $\text{La}_2\text{O}_3 : \text{Bi}^{3+}$ and europium co-doped sample.



The color of PL emissions observed from $\text{La}_2\text{O}_3:\text{Bi}^{3+}, \text{Eu}^{3+}$ powder samples changed to blue color from green colour as the temperature of the powder increased. Fig.12 shows the CIE chromaticity color coordinates of PL emissions from $\text{La}_2\text{O}_3 : \text{Bi}^{3+}$ and Eu^{3+} phosphor powder samples. In particular, the color change in PL emission observed from $\text{La}_2\text{O}_3 : \text{Bi}^{3+}, \text{Eu}^{3+}$ phosphor material is explained as a result that the energy of excited electrons has efficiently transferred from the excited state of Bi^{3+} to that of Eu^{3+} ion. CIE color coordinates have been calculated and found to be (0.30, 0.51), (0.16, 0.20), (0.34, 0.40), (0.30, 0.24), (0.32, 0.52), (0.22, 0.26), (0.17, 0.21) and (0.18, 0.30) respectively for $\text{La}_2\text{O}_3:\text{Bi}^{3+}$ (700 °C), $\text{La}_2\text{O}_3:\text{Bi}^{3+}$ (900 °C), $\text{La}_2\text{O}_3 : \text{Bi}^{3+}, \text{Eu}^{3+}$ (700 °C), $\text{La}_2\text{O}_3 : \text{Bi}^{3+}, \text{Eu}^{3+}$ (900 °C) respectively.

CONCLUSIONS

In this paper we have successfully synthesized $\text{La}_2\text{O}_3 : \text{Bi}^{3+}\text{Eu}^{3+}$ nanophosphors material by polyol method. The XRD patterns exhibited a hexagonal structure, and the FTIR spectra confirmed the presence of OH⁻ group in all as prepared La_2O_3 undoped and doped samples. After heating the as prepared La_2O_3 and $\text{La}_2\text{O}_3:\text{Bi}^{3+}$ and Eu^{3+} co-doped samples, the XRD pattern con-

firmed the formation of the pure La_2O_3 hexagonal phase. The effect of heating on the morphology of $\text{La}_2\text{O}_3:\text{Bi}^{3+}$ doped and rare earth Eu^{3+} , co-doped were also examined by SEM and TEM. All the observed emission peaks in PL from $\text{La}_2\text{O}_3:\text{Bi},\text{Eu}^{3+}$ phosphor powder were assigned to either the broad emission originating from the transition in Bi^{3+} or the visible emission peaks originating transition from the Eu^{3+} ions. The shifting of emission from the samples on heating is clearly observed from the CIE color coordinates plot. Finally, from the above studies, we are able to suggest that the $\text{La}_2\text{O}_3:\text{Bi}^{3+}, \text{Eu}^{3+}$ nanophosphors powders are promising materials for application in the development of novel optical systems such as FEDs, cathode ray tubes, plasma display panels, fluorescent lamps, etc.

ACKNOWLEDGEMENT

One of the authors (Dr.K.Ramachandra Rao) is grateful to the UGC-SERO, Government of India for sanctioning the minor research project (No.F MRP-4500/14). The authors express their gratitude towards Dr.V.Sudarsan, BARC, Mumbai for providing Photoluminescence studies. Our sincere thanks to Dr.Ch. Masthanaiah, Principal, Government College (A), Rajahmundry for providing necessary research lab facilities.

REFERENCE

- [1] S. Valange, A. Beauchaud, J. Barrault, Z. Gabelica, M. Daturi, F. Can, (2007), *J. Catal*, 251, 113. [2] W.M. Yen, M.J. Weber, (2004), *Inorganic Phosphors*, CRC Press, New York. [3] R.K. Datta, (1967), *J. Electrochem. Soc.*, 114, 1137. [4] G. Blasse, A. Bril, (1968) , *J. Chem. Phys.* 48, 217. [5] S.S. Kale, K.R. Jadhav, P.S. Patil, T.P. Gujar, C.D. Lokhande, (2005), *Mater. Lett.*, 59, 3007. [6] Y.H. Wu, M.Y. Yang, A. Chin, W.J. Chen, C.M. Kwei, (2000) *IEEE Electron Dev. Lett.*, 21, 341. [7] G. Blasse, (1970), *J. Lumin.* 1 (2), 766. [8] A.K. Levine, F.C. Palilla, (1964), *Appl. Phys. Lett.*, 5, 118. [9] A. Bril, W.L. Wanmaker, (1964), *J. Electrochem. Soc.*, 111, 1363. [10] L. Brixner, (1967), *J. Electrochem. Soc.*, 114, 352. [11] R. Reisfeld, C.K. Jorgensen, in: K.A. Gschneidner Jr., L. Eyring (Eds.), (1987), *Handbook of the Physics and Chemistry of Rare Earths*, Elsevier, North Holland, . Chapter 58. pp. 1–90. [12]S. Sheik Saleem, T.K.K. Srinivasan, (1987), *Pramana*, 29, 87. [13] J.Liu,X.Y.Fei, X.B.Yu, Z.W.Tao, L.Z.Yang, S.P.Yang, (2007) , *J.Non-Cryst.Solids*, 353, 4697. [14] M.Mendez, J.J.Carvajal, Y.Cesteros, M.Aguilo, F.Diaz, A.Giguere, D.Drouin, E.M. Ferrero, P.Salagre, P.Formentin, J.Pallares, L.F.Marsal, (2010), *Opt.Mater*,32, 1686. [15]X.M.Liu, L.S.Yan, J.P.Zou, (2010), *J.Electrochem.Soc.*, P1, 157. [16] Ying Zhang, Muying Wu, W. F. Zhang, (2010), *Modern Physics Letters B*, Vol. 24, Nos. 4 & 5, 475–485 . [17] Toshihiro Miyata, Jun-ichi Ishino, Keiichi Sahara, Tadatsugu Minami, (2011), *Thin Solid Films*, 519, 8095–8099. [18] H. Lui, L. Wang, S. Chen, B. Zuo, (2007), *J. Lumin.* 126, 459. [19] H.Q. Liu, L.L. Wang, W. Huang, Z.W. Peng (2007), *Mater. Lett.*, 61, 1968. [20] W. C. Koehler, E. O. Wollan, (1953), *Acta Cryst*, 6, 741. [21] W.M. Yen, M.J. Weber, (2004), *Inorganic Phosphors*, CRC Press, New York. [22] R.K. Datta, (1967), *J. Electrochem. Soc.*, 114, 1137. [23] G. Blasse, A. Bril, (1968), *J. Chem. Phys.* 48, 217. [24] Kim J S, Park Y H, Kim S M, et al, 2005, *Solid State Commun*, 133: 445–448. [25]Haruki Fukada, Kouhei Ueda, Jun-ichi Ishino, Toshihiro Miyata, Tadatsugu Minami, (2010), *Thin Solid Films*, 518, 3067–3070. [26] R. S. Knox, (1963), *Theory of Excitons*, *Solid State Physics Supplements*, Academic Press, New York, [27] J.K. Park, S.M. Park, C.H. Kim, H.D. Park, S.Y. Choi, (2001), *J. Mater. Sci. Lett.*, 20, 2231. [28] W. Di, X. Wang, B. Chen, S. Lu, X. Zhao, (2005) , *J. Phys. Chem. B*, 109, 13154–13158. [29] Sk. Khaja Hussain, Goli Nagaraju, E. Pavitra, G. Seeta Rama Raju and Jae Su Yu , (2015), *Cryst Eng Comm*, 17, 9431. [30] Jie Liu, Xiaoyan Fei, Xibin Yu , Zhenwei Tao, Liangzhun Yang, Shiping Yang, (2007), *Journal of Non-Crystalline Solids*, 353, 4697–4701. [31] Lixin Song, Pingfan Du, JieXiong, Xiaona Fan,Yuxuejiao, (2012), *J.Lumin.*, 132, 171–174.